Radiation Dose Distributions in Normal Tissue Adjacent to Tumors Containing ^{131}I or ^{90}Y: The Potential for Toxicity

Richard B. Sparks, PhD[1]; Eric A. Crowe[1]; Franklin C. Wong, MD, PhD, JD[2]; Richard E. Toohey, PhD[3]; and Jeffry A. Siegel, PhD[4]

[1]CDE Dosimetry Services, Inc., Knoxville, Tennessee; [2]Department of Nuclear Medicine, M.D. Anderson Cancer Center, Houston, Texas; [3]Oak Ridge Institute for Science and Education, Oak Ridge, Tennessee; and [4]Nuclear Physics Enterprises, Cherry Hill, New Jersey

Given the relatively large tumor-absorbed doses reported for patients receiving radionuclide therapy, particularly radioimmunotherapy, and the relatively long pathlength of the nonpenetrating emissions of some radionuclides being used for these therapies, there exists the possibility of large absorbed doses to tissues adjacent to, surrounded by, or surrounding these tumors. Because tumors can occur adjacent to critical organs or tissues, such as arteries, nerves, pericardium, and the walls of the organs of the gastrointestinal tract, large absorbed doses to these normal tissues can lead to acute complications. **Methods:** In this study, the Monte Carlo radiation transport code MCNP4b was used to simulate the deposition of energy from emissions of 2 radionuclides of interest, ^{131}I and ^{90}Y, to assess the possible magnitude of the absorbed doses in tissues adjacent to tumors. Mathematic models were constructed to simulate situations that might occur, such as tumor wrapped around a small cylinder (e.g., a nerve or artery), tumor against a tissue (e.g., the pericardium or wall of any gastrointestinal tract organ), and tumor surrounded by any soft tissue. Tumor masses of 10, 20, and 40 g were used in each model. Depth dose distributions were calculated using Monte Carlo simulations of the radiation transport in these geometric models. **Results:** For tissues close to tumors containing ^{90}Y, the absorbed dose ranged from 24% of the absorbed dose in the tumor, for the case of tissues 1 mm from the tumor, to 103% of the absorbed dose in the tumor, for the case of small structures such as nerves or arteries surrounded by tumor. For tissues close to tumors containing ^{131}I, the absorbed dose ranged from 4% of the absorbed dose in the tumor, for the case of tissues 1 mm from the tumor, to 46% of the absorbed dose in the tumor, for the case of small structures such as nerves or arteries surrounded by tumor. **Conclusion:** This study showed that when absorbed doses to tumors are large, the absorbed dose to adjacent tissues can also be large, potentially causing unexpected toxicities.

Key Words: dosimetry; radioimmunotherapy; tumors; absorbed-dose profile; tissue toxicity

J Nucl Med 2002; 43:1110–1114

Received Oct. 15, 2002; revision accepted Mar. 25, 2002.

For correspondence or reprints contact: Richard B. Sparks, PhD, CDE Dosimetry Services, Inc., 7108 Wright Rd., Knoxville, TN 37931.

E-mail: rsparks@creativedevelopment.com

Radionuclide therapy, particularly radioimmunotherapy, is designed to deliver a cytocidal radiation dose to a variety of tumors while minimizing the dose to normal tissues. The dose-limiting toxicity for most of these therapies without hematopoietic stem cell support is myelosuppression (*1–4*), but other toxicities in organs such as the spleen and kidneys have been reported (*5*). In addition to toxicities caused by direct uptake of activity in organs and tissues, another possibility is toxicity caused by irradiation of tissues that contain little activity themselves but are adjacent to regions of high activity uptake and retention, such as tumors. Tumor doses as high as 18,000 cGy (*3*) and 24,000 cGy (*6*) have been reported for 2 different monoclonal antibodies chelated to ^{90}Y in patients enrolled in radioimmunotherapy clinical trials. This study evaluated the potential absorbed dose to normal tissues close to activity-containing tumors. Absorbed dose distributions in normal tissue adjacent to, surrounded by, or surrounding 10-, 20-, and 40-g tumor sources containing ^{131}I or ^{90}Y, such as might be expected in radioimmunotherapy, were determined using the Monte Carlo radiation transport code MCNP4b. Three mathematic models were created for each of the 3 tumor sizes, resulting in 9 distinct models. Emissions for both ^{131}I and ^{90}Y were simulated separately for each model. These models were constructed with appropriate geometries to simulate a spheric tumor surrounding a small cylinder (such as a nerve), a hemispheric tumor against a tissue (such as the pericardium or wall of any gastrointestinal tract organ), and a spheric tumor surrounded by soft tissue.

MATERIALS AND METHODS

Geometric Models

For the spheric tumor–cylindric target (e.g., nerve or small artery) mathematic model in which the tumor surrounds the tissue, the target nerve or artery was modeled as a 1-mm-diameter cylinder positioned along the central *x*-axis of the sphere. This cylinder was subdivided into a central cylinder and 2 cylindric shells so that the absorbed dose as a function of depth could be determined. The

absorbed dose was determined to a lengthwise central portion of the entire cylinder to remove edge effects. This lengthwise central portion was set equal in length to the radius of the sphere in which it was contained and was centered in the sphere. A cutaway view of this model is shown in Figure 1.

For the hemispheric tumor–cylindric target mathematic model in which the tumor is directly adjacent to normal tissue, the target tissues were modeled as successive cylindric disks at increasing distances from the flat side of the hemispheric source tumor. The radii of the disks were chosen as one half the radius of the hemispheric source to eliminate edge effects. A cutaway view of this model is shown in Figure 2.

For the spheric tumor–spheric target model in which the tumor is surrounded by tissue, the target tissues were modeled as successive concentric spheric shells at increasing distances from the center of the spheric source tumor. A cutaway view of this model is shown in Figure 3.

Radiation Transport Simulations

MCNP4b was used to calculate the absorbed fractions for the various target regions for all tumor source models to simulate the deposition of energy from ^{131}I and ^{90}Y within normal tissue close to the source tumors. The composition of the source and target regions was assumed to be that of soft tissue, with a density of 1.04 g/cm^3 (*7*). Each radionuclide was assumed to be uniformly distributed within the hemispheric or spheric source tumor. Emission energies and yields for ^{131}I and ^{90}Y were taken from Weber et al. (*8*). Full β-spectra were generated for the 2 radionuclides. For the photon simulations, sufficient numbers of histories were run such that the relative errors were $<$5% and $<$8% for ^{131}I and ^{90}Y, respectively. For ^{90}Y, the total photon contribution was $<$0.01% of the total dose in each target region. For the electron simulations, sufficient numbers of histories were run such that the relative errors were $<$5.6% and $<$7.5% for ^{131}I and ^{90}Y, respectively, for all target regions for which the electron dose was $>$1% of the source total dose. The MCNP4b relative error criterion for generally reliable results is $\leq$10% (*9*).

The MCNP4b energy deposition tally was used to calculate the total energy deposited in the various target regions for all tumor source models. Energy deposition was tallied in the successive normal tissue targets, which ranged in thickness from 0.005 to 0.21 cm. The tally results from the MCNP4b simulations were converted into absorbed fractions and depth dose profiles using the standard MIRD methodology (*10*).

RESULTS

Depth dose distributions in surrounding normal tissue for the 10-, 20-, and 40-g hemispheric and spheric tumor source volumes containing ^{131}I or ^{90}Y were calculated. The results are given in Tables 1–3 as the percentage of source dose for the combined electron and photon components as a function of distance into the normal-tissue target for ^{131}I and ^{90}Y. For the model of a spheric tumor surrounding a small cylindric target (Table 1), the depths are equal to the distance from the source–target interface to the center of the respective cylindric shell (i.e., the distance into the normal-tissue target). For the model of a hemispheric tumor (Table 2), the depths are equal to the distance from the planar source–target interface to the center of the respective target disk (i.e., the distance into the normal-tissue target). For the model of a spheric tumor surrounded by spheric targets, the depths are equal to the distance from the center of the source

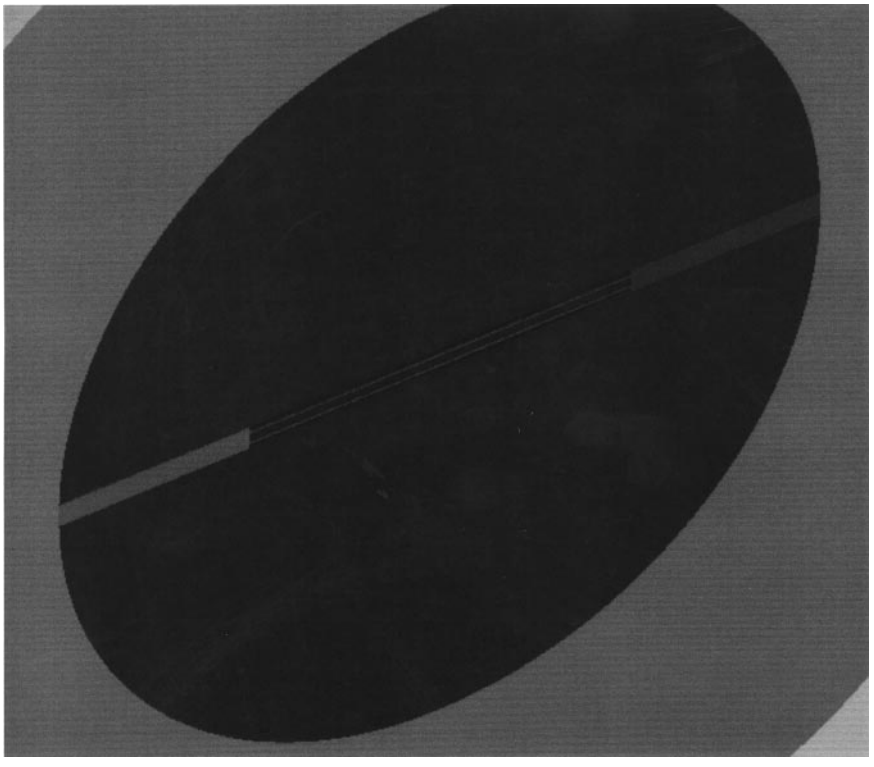

FIGURE 1. Cutaway view of spheric tumor–small cylindric target model.

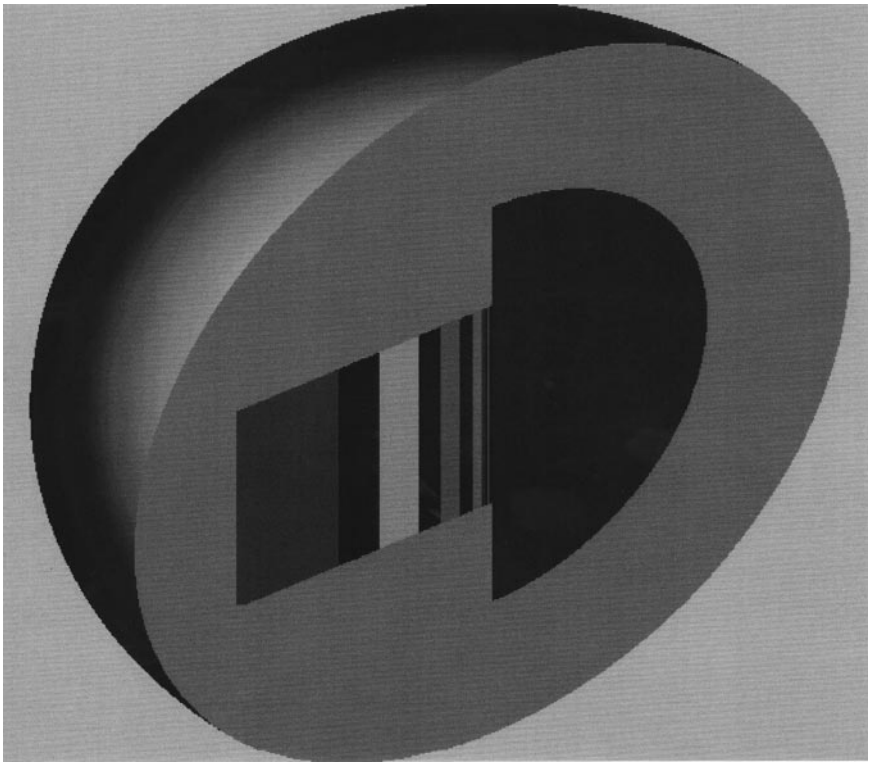

FIGURE 2. Cutaway view of hemispheric tumor–cylindric disk target model.

to the center of the respective target region minus the source radius (Table 3).

DISCUSSION

The depth dose distributions, that is, dose as a function of depth, in adjacent normal tissue were determined using the Monte Carlo radiation transport code MCNP4b for hemispheric and spheric tumors containing ^{131}I and ^{90}Y. The decrease in dose with distance from the tumor source was significantly greater for ^{131}I than for ^{90}Y. This finding is not surprising because the average range of the β-particles in soft tissue is 0.08 and 0.5 cm for ^{131}I and ^{90}Y, respectively.

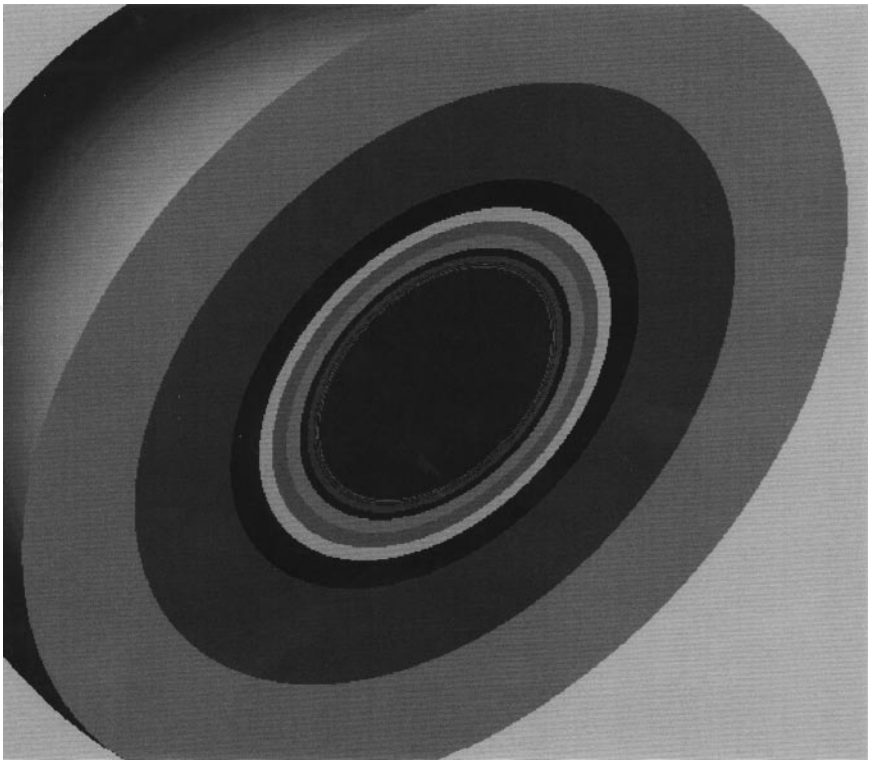

FIGURE 3. Cutaway view of spheric tumor–spheric shell target model.

TABLE 1
Depth Dose Profiles for ^{131}I and ^{90}Y in Tissue Adjacent to Spheric Tumor–Cylindric Target Model

	% Source dose					
	10-g tumor		20-g tumor		40-g tumor	
Depth (cm)	^{131}I	^{90}Y	^{131}I	^{90}Y	^{131}I	^{90}Y
Source	100	100	100	100	100	100
0.0085	50	104	51	102	52	98
0.025	36	103	37	98	39	95
0.042	31	100	31	99	35	96
S-value in source (μGy/MBq·s)	3.15	12.76	1.58	6.53	0.83	3.38

Tumors containing radioactivity can deliver a radiation dose to nearby normal tissues. The absorbed dose will vary with tumor activity uptake and retention and with radionuclide. If tumor-absorbed doses are known, the absorbed doses to adjacent tissues in geometries similar to those described in this study can easily be determined using Tables 1, 2, or 3. As can be seen from the tables, the dose to normal tissues is significantly less for ^{131}I than for ^{90}Y when tumor-absorbed doses are similar, but either could cause unexpected toxicities when tumor-absorbed dose is large.

The dose absorbed by normal tissues is simply determined from the percentage of the tumor-absorbed dose at the required depth given in each table. For example, if the absorbed dose in a 20-g tumor containing ^{90}Y is determined to be 10,000 cGy and this tumor is surrounding a small nerve (Table 1), the dose to the center of the nerve (at a depth of 0.042 cm) will be approximately 9,900 cGy. For the same scenario in the case of ^{131}I, the dose to the center of the nerve would be approximately 3,100 cGy. These normal-tissue doses can be compared with known tolerance doses (TDs), which, in external-beam radiation therapy, express the tolerance of normal tissues to the therapy. The 2 most common TDs are TD 5/5 (the probability of 5% complication within 5 y from treatment) and TD 50/5 (the probability of 50% complication within 5 y). TD 5/5 and TD 50/5 for neuropathy after irradiation of whole peripheral nerves are 1,500 and 2,000 cGy, respectively (*11*), and for neuritis after irradiation of 10 cm of nerve are 6,000 and 10,000 cGy, respectively (*12*). Because the amount of nerve tissue irradiated by a surrounding tumor is much smaller than the amount on which the TDs are based, these TDs cannot be directly applied. However, they do give some indication of the absorbed dose levels at which toxicity may potentially be observed.

As a second example of the use of the tables in this study, consider that the absorbed dose to a 40-g hemispheric tumor adjacent to the small intestine wall was 10,000 cGy (Table 2). The absorbed dose at the center of the intestinal wall (a depth of 0.15 cm) (*13*) would be approximately 2,000 cGy for ^{90}Y and 600 cGy for ^{131}I. The TD 5/5 and the TD 50/5 for ulcer, perforation, and hemorrhage for irradiation of 100

TABLE 2
Depth Dose Profiles for ^{131}I and ^{90}Y in Tissue Adjacent to Hemispheric Tumor–Cylindric Target Model

	% Source dose					
	10-g tumor		20-g tumor		40-g tumor	
Depth (cm)	^{131}I	^{90}Y	^{131}I	^{90}Y	^{131}I	^{90}Y
Source	100	100	100	100	100	100
0.0025	46	61	46	58	47	56
0.01	32	56	33	54	34	52
0.02	22	52	24	50	24	48
0.03	17	48	18	46	19	44
0.04	13	44	14	42	15	41
0.05	10	42	11	39	12	38
0.06	8	39	9	37	10	36
0.07	7	36	8	35	9	34
0.08	6	34	7	33	8	31
0.09	5	32	6	31	8	30
0.10	5	30	6	28	7	28
0.15	4	22	5	21	6	20
0.25	3	11	4	11	6	11
0.40	3	4	4	4	5	4
0.60	2	1	3	1	4	1
S-value in source (μGy/MBq·s)	3.15	12.00	1.58	6.38	0.83	3.30

TABLE 3
Depth Dose Profiles for ^{131}I and ^{90}Y in Tissue Adjacent to Spheric Tumor–Spheric Target Model

	% Source dose					
	10-g tumor		20-g tumor		40-g tumor	
Depth (cm)	^{131}I	^{90}Y	^{131}I	^{90}Y	^{131}I	^{90}Y
Source	100	100	100	100	100	100
0.0025	43	53	43	52	44	52
0.01	31	48	31	48	32	48
0.02	21	44	21	43	22	44
0.03	15	40	16	40	17	40
0.04	11	37	12	37	13	37
0.05	8	35	9	34	11	34
0.06	7	32	8	32	9	32
0.07	5	30	6	30	7	30
0.08	5	28	6	28	7	28
0.09	4	26	5	26	6	26
0.10	4	24	5	24	6	24
0.15	3	17	4	17	5	17
0.25	2	8	3	8	4	9
0.40	2	3	3	3	4	3
0.60	2	0.4	2	0.4	3	0.4
S-value in source (μGy/MBq·s)	3.15	12.75	1.58	6.53	0.83	3.38

cm^2 of intestine are 5,000 and 6,500 cGy, respectively (*12*). The caveat regarding whole and partial irradiation mentioned in the first example applies here as well.

CONCLUSION

Because the radiation dose to normal tissues close to activity-containing tumors can be quite large, potential toxicities may occur, especially for particularly radiosensitive tissues. Because of the larger maximum β-emission energy and longer emission pathlength of ^{90}Y, absorbed dose to adjacent tissues falls off more slowly as a function of depth from tumors containing ^{90}Y than from tumors containing ^{131}I. For example, using the hemispheric model, the absorbed dose in the tissues adjacent to a 20-g tumor are reduced to roughly 25% of the tumor-absorbed dose at 0.2 and 1 mm for ^{131}I and ^{90}Y, respectively. Thus, unexpected toxicities to adjacent tissues will likely occur more frequently with ^{90}Y than with ^{131}I if tumor doses for the 2 radionuclides are similar.

ACKNOWLEDGMENT

This article describes activities performed under contract DE-AC05-00OR22750 between the U.S. Department of Energy and Oak Ridge Associated Universities (Oak Ridge, TN). The Oak Ridge Institute for Science and Education (ORISE) is a U.S. Department of Energy facility focusing on scientific initiatives to research health risks from occupational hazards, assess environmental cleanup, respond to radiation medical emergencies, support national security and emergency preparedness, and educate the next generation of scientists. ORISE is managed by Oak Ridge Associated Universities. Accordingly, the U.S. government retains a nonexclusive, royalty-free license to publish or reproduce the published form of the contribution, or allow others to do so, for U.S. government purposes.

REFERENCES

1. Kairemo KJ. Radioimmunotherapy of solid cancers: a review. *Acta Oncol.* 1996;35:343–355.
2. O'Donnell RT, DeNardo SJ, Yuan A, et al. Radioimmunotherapy with $^{111}In/^{90}Y$-2IT-BAD-m170 for metastatic prostate cancer. *Clin Cancer Res.* 2001;7:1561–1568.
3. Richman CM, DeNardo SJ. Systemic radiotherapy in metastatic breast cancer using ^{90}Y-linked monoclonal MUC-1 antibodies. *Crit Rev Oncol Hematol.* 2001; 38:25–35.
4. Kaminski MS, Fig LM, Zasadny KR, et al. Imaging, dosimetry, and radioimmunotherapy with iodine 131-labeled anti-CD37 antibody in B-cell lymphoma. *J Clin Oncol.* 1992;10:1696–1711.
5. Cremonesi M, Ferrari M, Chinol M, et al. Dosimetry in radionuclide therapies with ^{90}Y-conjugates: the IEO experience. *Q J Nucl Med.* 2000;44:325–332.
6. Wiseman GA, White CA, Sparks RB, et al. Biodistribution and dosimetry results from a phase III prospectively randomized controlled trial of Zevalin radioimmunotherapy for low-grade, follicular, or transformed B-cell non-Hodgkin's lymphoma. *Crit Rev Oncol Hematol.* 2000;39:181–194.
7. Cristy M, Eckerman KF. *Specific Absorbed Fractions of Energy at Various Ages from Internal Photons Sources.* Oak Ridge, TN: Oak Ridge National Laboratory; 1987:79. ORNL/TM-8381 V1.
8. Weber DA, Eckernan KF, Dillman LT, et al. *MIRD: Radionuclide Data and Decay Schemes.* Reston, VA: Society of Nuclear Medicine; 1989:159, 229.
9. *RSICC MCNP Manual: Monte Carlo N-Particle Transport Code System.* Los Alamos, NM: Los Alamos National Laboratory; 1994:2–93.
10. Loevinger R, Budinger TF, Watson EE. *MIRD Primer*. Reston, VA: Society of Nuclear Medicine; 1999:5–6.
11. Rubin P. Law and order of radiation sensitivity: absolute versus relative. *Front Radiat Ther Oncol.* 1989;23:7–40.
12. Bentel GC, Nelson CE, Noell KT. *Treatment Planning and Dose Calculation in Radiation Oncology*. 4th ed. Elmsford, NY: Pergamon Press; 1989:3–6.
13. Synder WS, Cook MJ, Nasset ES, Karhausen LR, Howells GP, Tipton IH. *International Commission on Radiological Protection No. 23 (ICRP-23) Report of the Task Group on Reference Man.* New York, NY: Pergamon Press; 1975: 139–140.